

Carbon – platinum nanostructured catalysts for hydrogen fuel cells

L. PETRĂȘESCU^{a*}, V. CIUPINĂ^{a,d}, Ș. G. TUTUN^b, R. VLĂDOIU^a, G. PRODAN^a, C. POROȘNICU^c, E. VASILE^c, I. PRIOTEASA^b, R. MANU^b

^a"Ovidius" University of Constanta, Mamaia 124, Constanta, 900527, Romania

^bFaculty of Physics, University of Bucharest, Atomistilor 405, Măgurele, Ilfov

^cNational Institute for Laser, Plasma and Radiation Physics, PO Box MG-36, 077125, Bucharest, Romania

^dAcademy of Romanian Scientists, Independenței 54, Bucharest 050094, Romania

^eUniversity „Politehnica” of Bucharest, No. 1-7 Gh. Polizu Street, Bucharest 011061, Romania

As the necessity for energy keeps on growing it has become a pressing concern the development of new methods of producing energy both efficient and harmless for our environment. In the past the limiting factors of renewable energy were the storage and transport of that energy. By using fuel cells and hydrogen based technology the electrical energy from renewable sources can be distributed where and when is needed, clean, efficient and sustainable. Nanotechnology is the area of interest in the research of new methods of improving the performance and reducing the costs of the catalysts used in fuel cells [1, 2, 3, 4]. In order to prepare nanostructured carbon based films (C – Glass + Pt) for use in the anode and cathode parts of fuel cells, the method of Thermionic Vacuum Arc (TVA) was used in one electronic gun configuration. One of the main advantages of this technology is the bombardment of the growing thin film just by the ions of the depositing material. Moreover, the energy of ions can be controlled. Thermo-electrons emitted by an externally heated cathode and focused by a Wehnelt focusing cylinder are accelerated towards the anode whose material is evaporated and bright plasma is ignited by a high voltage DC supply [5]. The nanostructured C – Glass + Pt films were characterized by Transmission Electron Microscopy (TEM), electron diffraction, Scanning Electron Microscopy (SEM), Energy Dispersive X-Ray Spectrometry (EDXS) and magneto-resistance analysis. In the presence of a magnetic field of 0.3 T all the films that were investigated showed a slight drop in resistance. The TEM analysis showed the investigated films have a uniform morphology and amorphous structure, SEM also revealed the uniform character of the surface while EDXS confirmed the presence of Platinum.

(Received December 11, 2014; accepted September 9, 2015)

Keywords: C – Glass + Pt, TEM, SEM, electron diffraction, EDXS, TVA, Magnetoresistance, fuel cells

1. Introduction

Fuel Cells are devices that convert chemical energy from a fuel such as hydrogen into electricity through chemical reactions with oxygen or other oxidizing agents and are advantageous for compact applications as they can replace static energy sources such as Li-ion batteries by providing longer lifetimes and higher energy densities [6].

The source of energy for these cells is situated at the anode, the oxidant at the cathode while the electrolyte allows the ions to flow between these two parts of the fuel cell. The most common type of fuel used is hydrogen but hydrocarbon fuel such as natural gas or alcohols like methanol are also used. However, such fuel cells require either on-site hydrogen storage or an onboard reformer to extract H₂ from organic fuels [6].

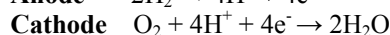
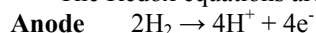
A catalyst is required for the oxidation of a fuel such as hydrogen and platinum-based catalysts are the most efficient but are also very expensive. While Pt is an excellent catalyst for dehydrogenation it is extremely susceptible to poisons such as carbon monoxide (CO) present in the hydrogen gas obtained by reforming hydrocarbon fuel [7]. Complex alloys of Pt and various

metals such as Mo, W, Re, Rh and Pd are also explored as fuel cell electro-catalysts [8] while efforts have also been devoted to the optimization of the existing platinum nanoparticle catalysts and to the design of new catalysts with less or no usage of Pt [9,10].

Unlike batteries, fuel cells need to be always connected to the fuel source and to oxygen to produce low voltage electrical current. Individual cells produce low amounts of electricity (aprox. 0.7-0.9V) that's why they are stacked in series or parallel circuits to satisfy the power requirements of various applications [11].

At the anode of a hydrogen fuel cell weak H – Pt bonds are formed. The H atoms are oxidized so their electrons travel to the cathode through the external electric circuit. The remaining H proton is linked with a water molecule from the electrolyte membrane and forms a hydronium ion H₃O⁺ which travels to the cathode. At the cathode weak O – Pt bonds are formed. The O atoms from the air are reduced and by combining with the H protons from the anode water molecules are formed.

The Redox equations are as follows:



Total $2\text{H}_2 + \text{O}_2 \rightarrow 2\text{H}_2\text{O}$ [12].

2. Materials and methods

The C–Pt thin films on Glass substrate have been obtained by Thermionic Vacuum Arc method [5] (**Fig.1**) and the deposition consisted of two stages: the carbon deposition (filament current intensity had a value of **38A** for the whole **37 min** deposition time and the rate was 0.2 – 0.3 Angstrom/s on Glass substrate resulting in a Carbon thickness of about **50nm**) and the platinum deposition (filament current intensity had a value of **35.9A** for the whole **13 min** deposition time and the rate was 0.05 Angstrom/s on C – Glass resulting in isles of Pt with thicknesses ranging from **3.2 – 4nm** (**Fig. 2**) (**Table 1**)).

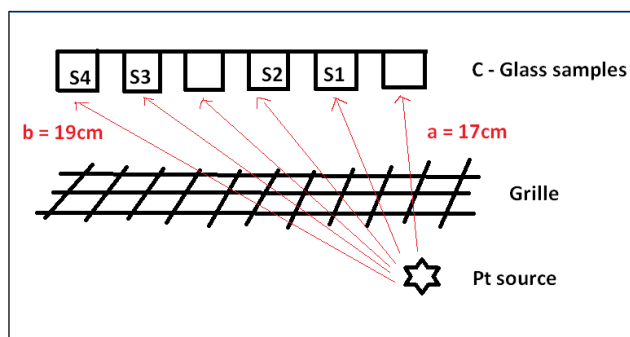


Fig. 1. The TVA deposition arrangement

Four thin film samples (S1, S2, S3 and S4) were investigated using electrical analysis while samples S1 and S3 undergone further TEM, SEM, EDXS measurements for morphology, crystalline structure and physical properties.

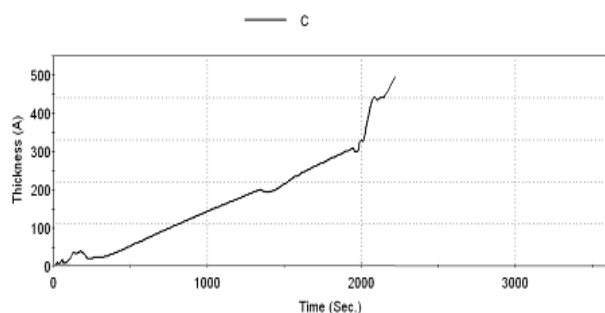


Fig. 2a – Carbon deposition (Thickness [Å] vs. Time [sec]).

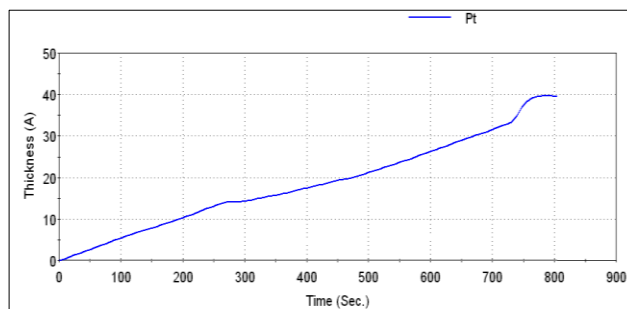


Fig. 2b – Platinum deposition (Thickness [Å] vs. Time [sec])

Tab. 1 – Thickness of the samples S1, S2, S3 and S4

Sample	Estimated Thickness (nm)
S1	3.8
S2	3.6
S3	3.3
S4	3.2

Ohmic contacts were attached on the samples for use in the electrical measurements. The electrical contact on the samples was performed by a product consisting of 80% silver-filled two-component epoxy-based glue (0.0025 Ω/cm specific resistance) [13].

TEM was performed using the Philips CM120ST microscope with MegaView III CSD camera. SEM analysis used the SEM QUANTA INSPECT F. Samples S1 and S3 were prepared using the scratch method.

3. Results and discussions

Fig.3a and Fig.3b illustrates the TEM morphological images and electron diffraction analysis of samples S1 and S3 respectively.

The TEM analysis reveals that all investigated films have a uniform morphology and amorphous structure.

The TEM image of sample S1 shows the formation of platinum polycrystalline structures on the surface of the thin film. Instead, sample S3 reveals a film like structure for platinum (these implications will be further explored when we reach the electrical measurements).

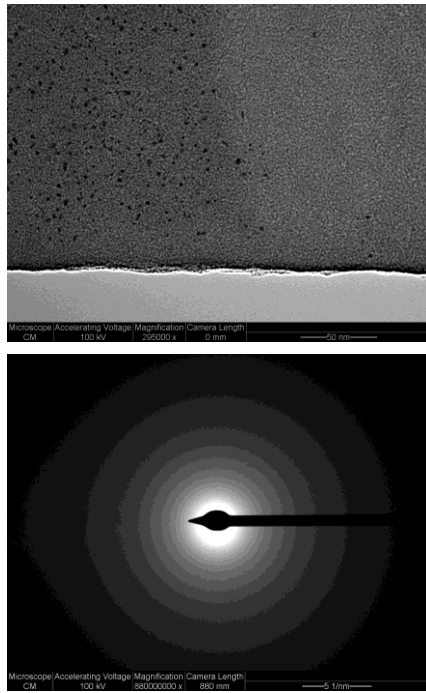


Fig.3a TEM and electron diffraction analysis of sample S1

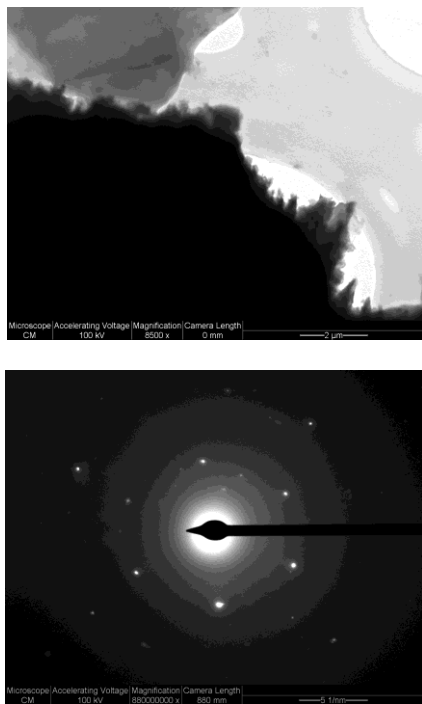


Fig.3b TEM and electron diffraction analysis of sample S3

SEM analysis for samples S1 and S3 is presented in Fig.4 and Fig.5 respectively.

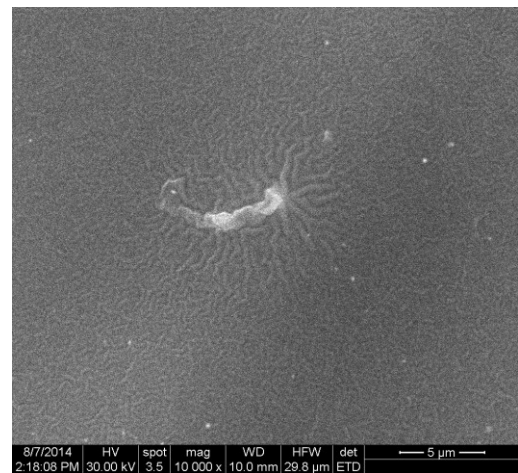
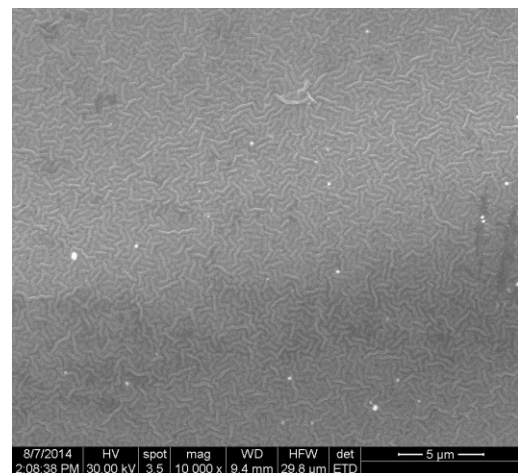
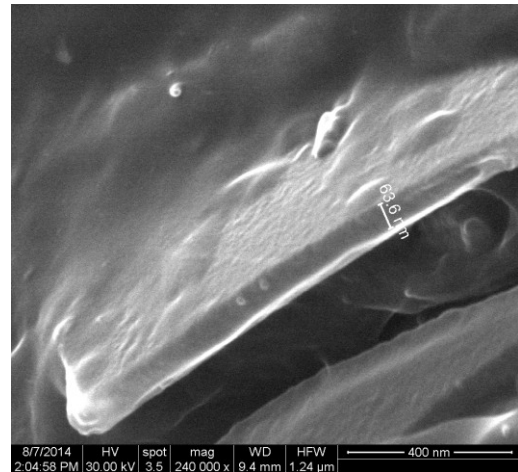


Fig.4 SEM analysis for Sample 1 with varying magnification (240.000x - top, 10.000x – middle and bottom) On the first image (240.000x - top) we can actually measure the width of the C – Pt film to be 63.6 nm.

Proceeding to the next two images we can observe the uniform but also the vermicular aspect of the deposited thin film.

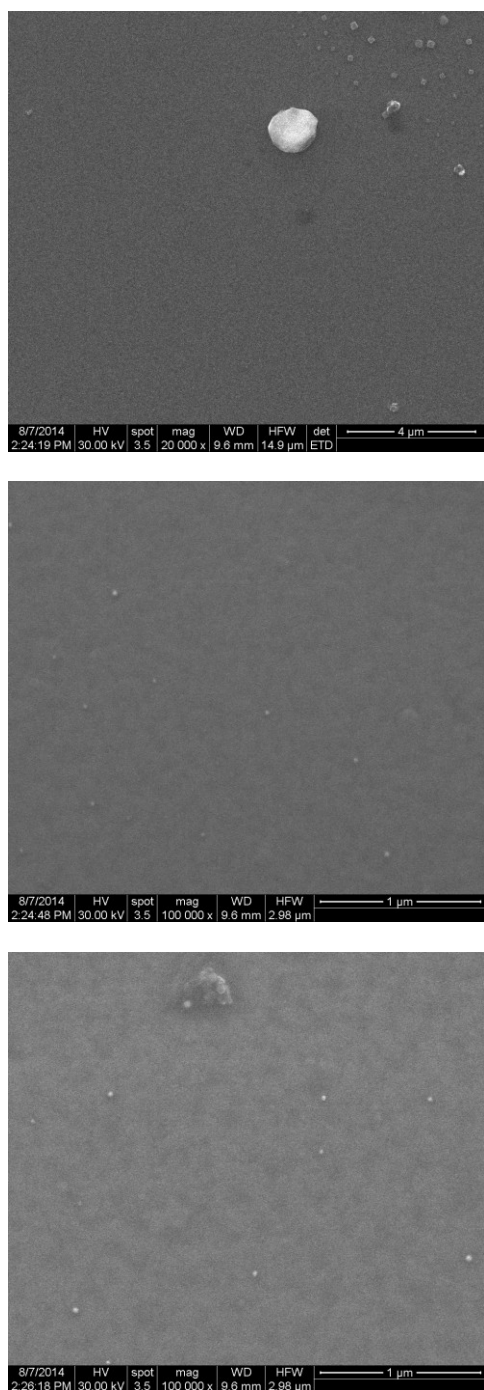


Fig.5 SEM analysis for sample S3 with varying magnification (20.000x - top, 100.000x – middle and bottom)

All images illustrate a uniform surface of the film. This sample does not show the same pronounced vermicular character as sample S1 (middle and bottom images) and has occasional large impurities of about 1 μm in diameter (top image).

The EDAX analysis (Fig. 6) confirms the presence of C and Pt in samples S1 and S3. In the examined portions of the two samples we can qualitatively say that Pt is more defined and in higher quantities in sample S1 at energies of 1.7, 2.1 and 2.4 keV. Also we can observe the presence of oxygen, calcium, sodium and magnesium on the surface of the films.

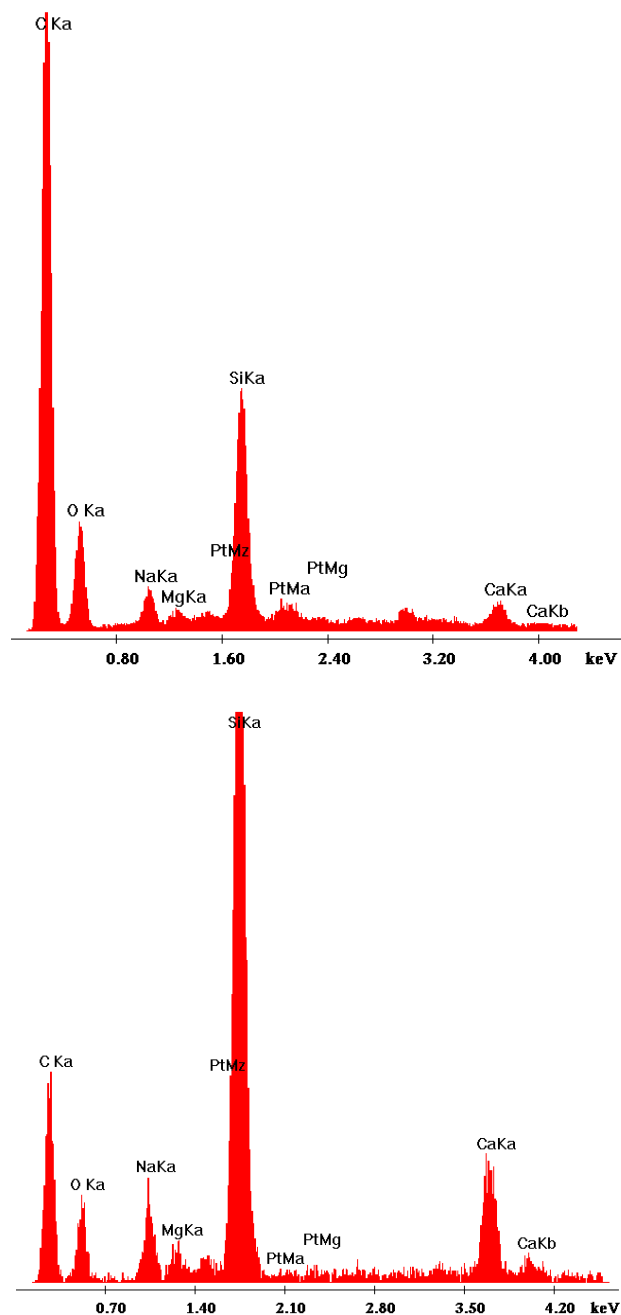


Fig.6 EDXS analysis for sample S1 (top) and sample S3 (bottom)

Electrical measurements investigate the conductivities of samples S1, S2, S3 and S4. Resistance of the samples was measured comparing the potential drop on the sample with the potential drop on a standard series resistance in constant current mode [13].

It can be seen in Fig.7 how the resistance of sample S1 which has a thickness of about 3.8nm is affected by temperature and magnetic field intensity applied perpendicular to the surface of the sample.

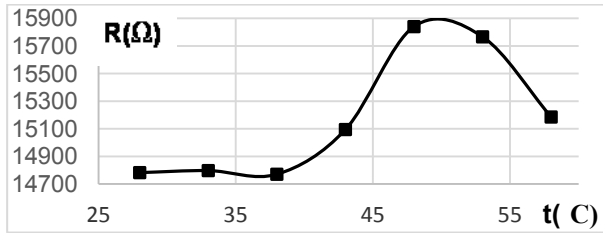


Fig.7a – Sample S1 resistance vs. temperature graph

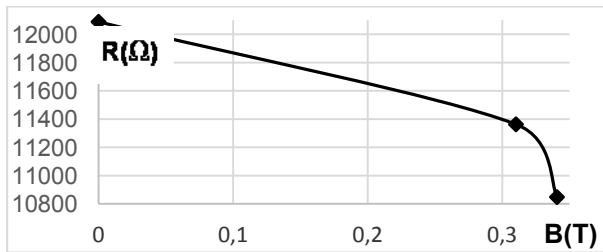


Fig.7b – Sample S1 resistance vs. magnetic field intensity graph

Fig.8a, 8b and 8c shows the resistance vs. temperature graph for samples S2, S3 and S4 respectively without a magnetic field and with a magnetic field of 0.3102 Tesla.

It can be seen that in the presence of that magnetic field perpendicular to the surface of the sample all the structures that were investigated showed a slight drop in resistance.

Fig.9 shows a comparison between all 4 samples in a resistance per distance between contacts vs. temperature graph.

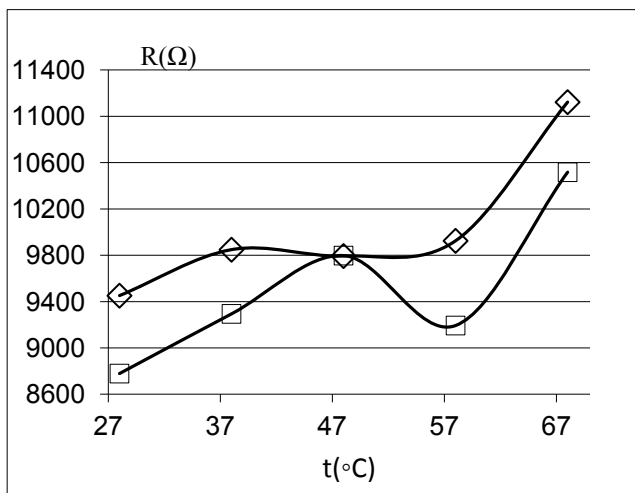


Fig.8a – Sample S2 resistance vs. temperature graph, (◇) null magnetic field, (□) magnetic field B=0.3102T

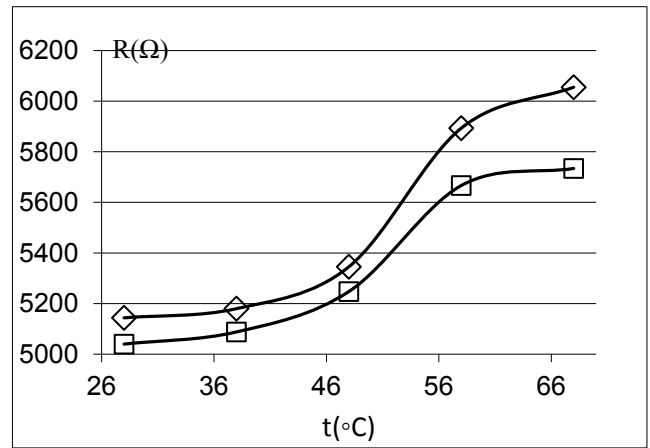


Fig.8b . Sample S3 resistance vs. temperature graph, (◇) null magnetic field, (□) magnetic field B=0.3102T

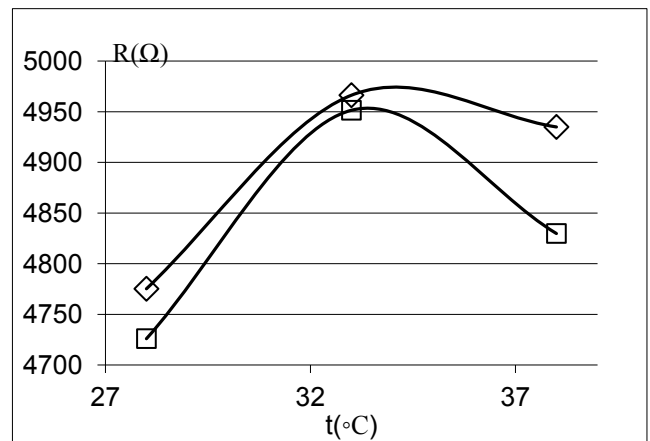


Fig.8c. Sample S4 resistance vs. temperature graph, (◇) null magnetic field, (□) magnetic field B=0.3102T

The magnetoresistance MR(%) in a magnetic field of intensity B=0.3102T vs. temperature for samples S2, S3 and S4 is presented in Table 2.

Tab. 2 – MR (%) vs. temperature (B=0.3102T)

t(°C)	MR (%)		
	Sample S2	Sample S3	Sample S4
28	-7.11	-2.02	-1.03
33			-0.3
38	-5.63	-1.78	-2.13
48	0.04	-1.84	
58	-7.37	-3.85	
68	-5.44	-5.31	

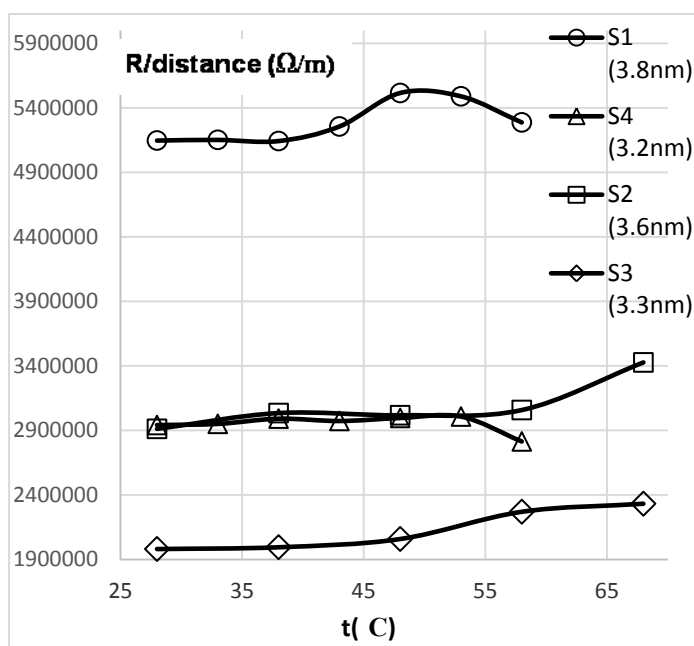


Fig.9. Resistance – distance ratio vs. temperature for sample S1(\circ), sample S4(Δ), sample S2(\square) and sample S3(\diamond)

It can be seen that sample S1 even if it has isles of Pt with thickness of 3.8nm has the highest resistance per distance ratio of all 4 samples. By contrast sample S3 with only 3.3nm has the lowest ratio of all.

These measurements lead to the conclusion that it is the surface of Pt between contacts which decreases the resistance.

The lower resistance per distance results for sample S3 compared to sample S1 from the resistance analysis are in agreement with the previous TEM analysis which revealed the formation of platinum polycrystalline structures on the surface of sample S1 while sample S3 presented a film like structure.

4. Conclusions

The nanostructured C – Glass + Pt films were obtained by TVA method. Such nanostructures were characterized by Transmission Electron Microscopy (TEM), electron diffraction, Scanning Electron Microscopy (SEM), Energy Dispersive X-Ray Spectrometry (EDXS) and electrical analysis. The TEM analysis revealed the films have a uniform morphology and amorphous structure and in the case of sample S3 Pt forms a film like structure. The resistance / distance graph shows that it is the surface of Pt between contacts that determines the decrease in resistance. In the presence of a magnetic field perpendicular to the surface of the nanostructures, all the films showed a slight drop in resistance.

References

- [1] V. Ciupina, I. G. Morjan, R. Alexandrescu, et al., Proceedings of SPIE Vol. **7764**, 77640O (2010);
- [2] I. Jepu, C. Porosnicu, C.P. Lungu, I. Mustata, C. Luculescu, V. Kuncser, G. Iacobescu, A. Marin, V. Ciupina, Surf. Coat. Technology, **240**, 344 (2014)
- [3] V. Kuncser, G. Schinteie, P. Palade, I. Jepu, I. Mustata, C.P. Lungu, F. Miculescu, G. Filoti Journal of Alloys and Compounds, **499**(1), 23 (2010).
- [4] V. Stancu, C. Dragoi, V. Kuncser, G. Schinteie, L. Trupina, E. Vasile, L. Pintilie, Thin Solid Films, **519**(19), 6269 (2011).
- [5] G. Musa, I. Mustata, V. Ciupina, R. Vladoiu, G. Prodan, E. Vasile, H. Ehrich Diem.Rel.Mat. **13**, 1398 (2004)
- [6] C. L. Lamy, J.-M; Srinivasan, S. Direct Methanol Fuel Cells: From a Twentieth Century Electrochemist's Dream to a Twenty-first Century Emerging Technology; Kluwer Academic/Plenum Publishers: New York, 2001; Vol. 34.
- [7] Emerilis Casado-Rivera, David J. Volpe, Laif Alden, Cora Lind, Craig Downie, Terannie Vazquez-Alvarez, Antonio C. D. Angelo, Francis J. DiSalvo, Hector D. Abruna. Electrochemical Activity of Ordered Intermetallic Phases for Fuel Cell Applications; JACS Articles; Published on Web 03/06/2004
- [8] Hogarth, M. P.; Ralph, T. R. Platinum Metals Rev. **46**, 146 (2002).

- [9] (a) H. Lee, S. E. Habas, S. Kwekin, D. Butcher, G. A. Somorjai, P. Yang, *Angew. Chem., Int. Ed.* **45**, 7824 (2006) (b) Ren, J.; Tilley, R. D. *J. Am. Chem. Soc.* **129**, 3287. (2007) (c) C. Wang, H. Daimon, T. Onodera, T. Koda, S. Sun, *Angew. Chem., Int. Ed.*, **47**, 3588 (2008).
- [10] (a) B. Lim, M. Jiang, P. H. Camargo, E. C. Cho, J. Tao, Lu, X.; Zhu, Y.; Xia, Y. *Science*, **324**, 1302. 2009 (b) Z. Peng, H. Yang, *J. Am. Chem. Soc.* **131**, 7542. (2009) (c) M. Lefevre, E. Proietti, F. Jaouen, J.-P. Dodelet, *Science*, **324**, 71 (2009).
- [11] http://chemwiki.ucdavis.edu/Analytical_Chemistry/Electrochemistry/Case_Studies/Commercial_Galvanic_Cells
- [12] W. R. Grove, *Philosophical Magazine* and *Journal of Science* **13**, 430 (1838).
- [13] V. Ciupina, C. P. Lungu, R. Vlădoiu, G. C. Prodan, S. Antohe, C. Porosnicu, I. Stanescu, I. Jecu, S. Iftimie, M. Prodan, A. Mandes, V. Dinca, E. Vasile, V. Zarovski, V. Nicolescu, *Proceedings of SPIE Vol. 9172, NANOSTRUCTURED THIN FILMS VII*, San Diego, California, United States (20-21 August 2014).

*Corresponding author: ronin4862@yahoo.com